Supplementary Information

Engineering one-dimensional trough-like Au–Ag_2S nano-hybrids for plasmon-enhanced photoelectrodetection of human α-thrombin

Wen-Chao Geng, [a] De-Lin Li, [a] Ji-Long Sang, [a] Liang-Liang Pan, [a] Ze-Li Jiang, [a] Cai Liu, *[b] Yong-Jun Li *[a]

[a]State Key Lab of Chemo/Biosensing and Chemometrics, College of Chemistry and Chemical Engineering, Hunan University, Changsha 410082, China. E-mail: liyje@hnu.edu.cn

[b]College of Chemical Engineering, Beijing Institute of Petrochemical Technology, Beijing 102617, China. E-mail: liucai@bipt.edu.cn

Experimental

Synthesis of Ag nanowires. Silver nanowires were prepared by a previously reported polyol process.[1,2] Typically, ethylene glycol (EG, 10.0 mL) after refluxed at 196 ^{o}C for 5 h was cooled to 160 ^{o}C, to which were added two EG solutions at the same rate of 0.2 mL·min^{-1} under vigorous stirring: $AgNO_3$ (5.0 mL, 0.2 mol·L^{-1}) and PVP (5.0 mL, 0.3 mol·L^{-1}). After ~ 45 min, the solution color gradually turned from bright yellow to gray, indicative of the formation of Ag nanowires. The resulting Ag nanowires were collected by centrifugation, washed successively with acetone and water to remove excess PVP and EG, and redispersed in ethanol (250.0 mL) for further use.

Optimization of DNA modification to ITO/Au–Ag_2S

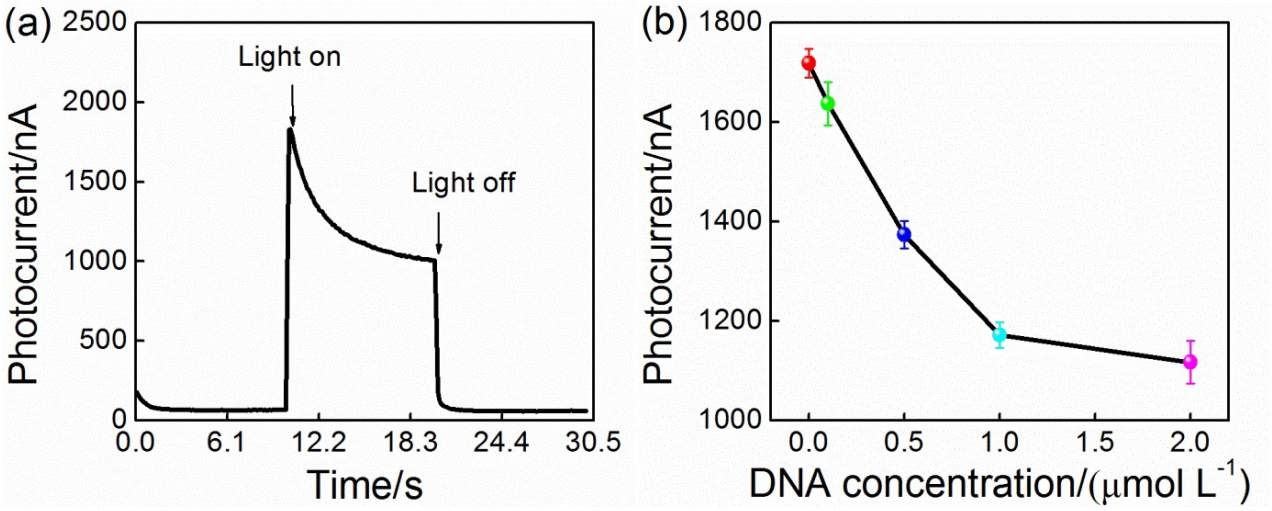

Fig. S1 (a) Photocurrent responses of ITO/Au–Ag_2S in 0.10 mol·L^{-1} Tril–HCl (pH 7.4) containing 0.10 mol·L^{-1} ascorbic acid; (b) Maximum photocurrent of ITO/Au–Ag_2S modified with 20 μL of DNA solution (i.e., ITO/Au–Ag_2S/DNA) with different concentrations in 0.10 mol·L^{-1} Tril–HCl (pH 7.4) containing 0.10 mol·L^{-1} ascorbic acid.

The ITO/Au–Ag_2S electrode shows a remarkable phothocurrent, as shown in **Fig. S1a**. When DNA molecules were modified to 1D Au–Ag_2S nanotroughs, the photocurrent decreased because of the blocking effect of the poor-conductive DNA. **Fig. S1b** shows the correlation between DNA concentrations and photocurrent. When the DNA concentration changed from 1.0 to 2.0 μmol·L^{-1}, the photocurrent did not show a big change, indicative of saturated immobilization of DNA on the surface of Au–Ag_2S. Therefore, the DNA concentration was fixed at 1.0 μmol·L^{-1} for the fabrication of ITO/Au–Ag_2S/DNA, as described in Experimental Section of body text.

Blocking of nonspecific binding sites of ITO/Au–Ag_2S/DNA

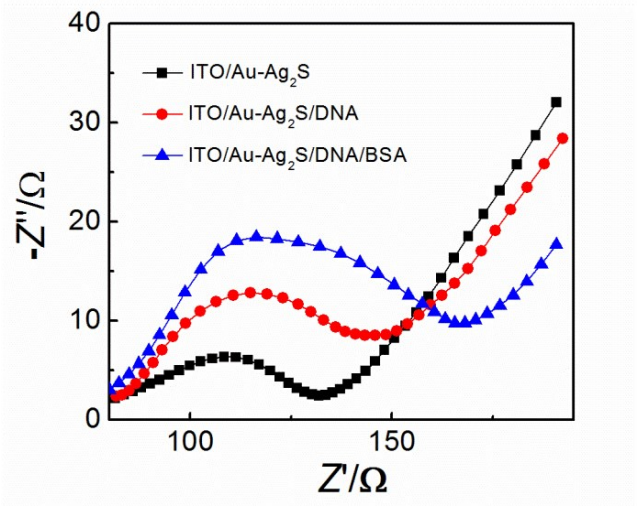

Fig. S2 Nyquist plots of different electrodes in 0.10 mol·L^{-1} KCl aqueous solution containing 5.0 mmol L^{-1} $[Fe(CN)_6]^{3-}$ at −0.22 V (0.1 Hz–100 kHz; amplitude, 5 mV).

To block the remaining active sites of ITO/Au–Ag_2S/DNA, 20 μL of BSA aqueous solution (1.0 wt%) was added on ITO/Au–Ag_2S/DNA by a drop-coating method. Successful modification of DNA and BSA can be confirmed by electrochemical impedance spectroscopy (EIS), as shown in **Fig. S2.** In Nyquist plots of EIS, the semicircle diameter at high frequency is proportional to the interfacial charge-transfer resistance (R_{ct}) of the electrode.[3] **Fig. S2** shows that the R_{ct} values of ITO/Au–Ag_2S, ITO/Au–Ag_2S/DNA, and ITO/Au–Ag_2S/DNA/BSA electrodes were 50.2, 75.8, and 91.3 Ω, respectively, in $[Fe(CN)_6]^{3-}$ solution, indicative of the successful modification of DNA and BSA.

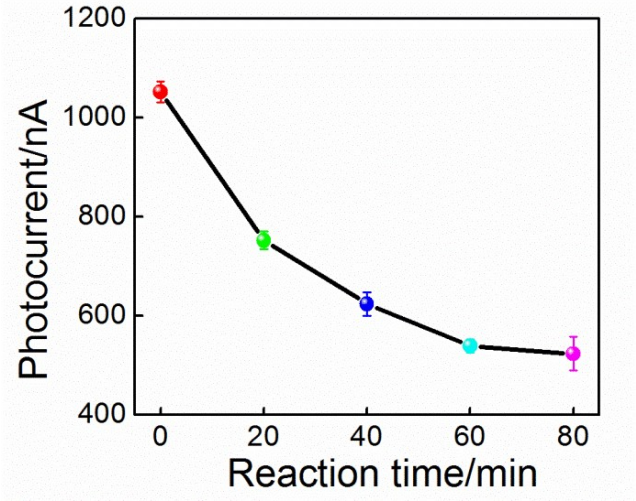

Fig. S3 Influence of the reaction time between TB (TB, 20 μL, 10.0 pmol·L^{-1}) and ITO/Au–Ag_2S/DNA/BSA on the photocurrent. The photocurrents were measured in 0.10 mol·L^{-1} Tril–HCl (pH 7.4) containing 0.10 mol·L^{-1} ascorbic acid.

When TB was specifically bound to the DNA of ITO/Au–Ag_2S/DNA/BSA, the photocurrent decreased (**Fig. S3**). When the reaction time reached 60 min, nearly all DNA reacted with TB and the photocurrent did not show a big change when the reaction time was more than 60 min. Thus, 60 min is choosen as the optimal reaction time in all TB detection analyses.

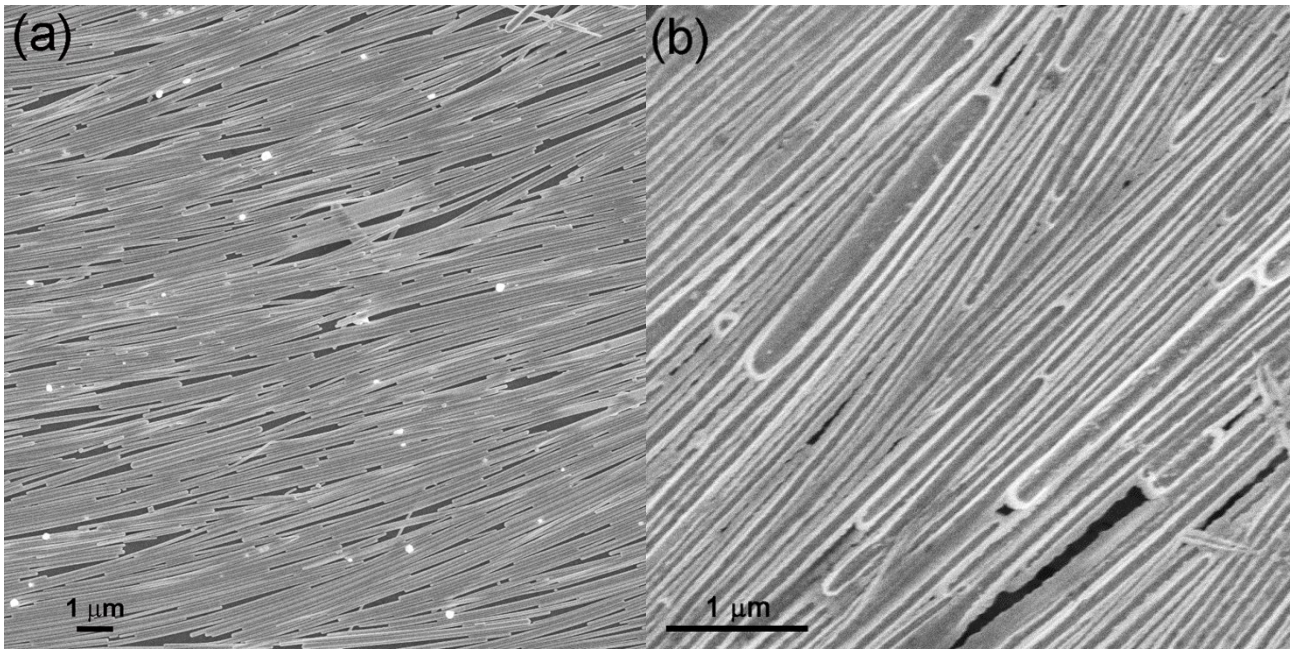

Fig. S4 SEM images of (a) Ag nanowires and (b) 1D AgAu nanotrough monolayer transferred onto silicon wafer.

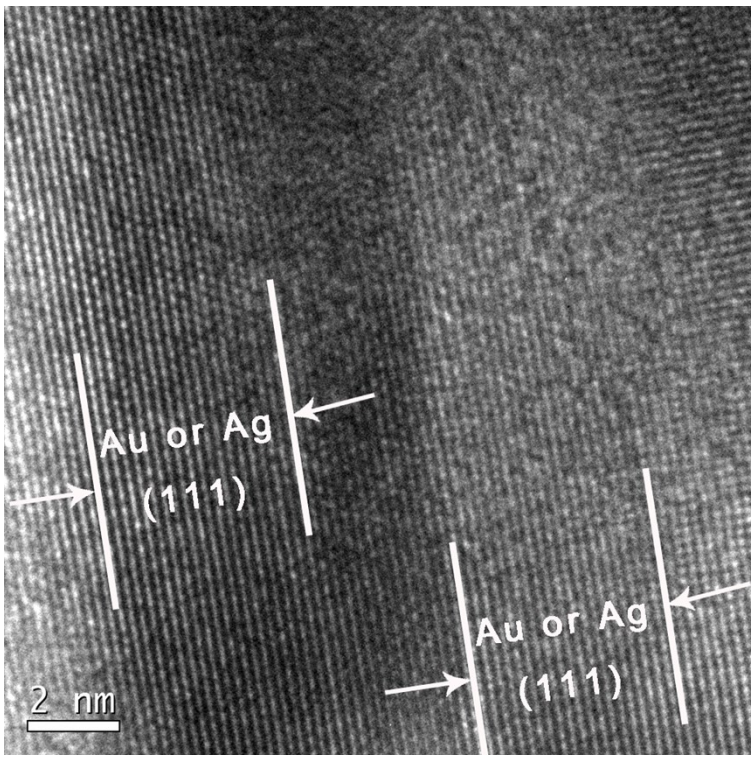

Fig. S5 HRTEM image of the 1D AgAu nanotrough wall.

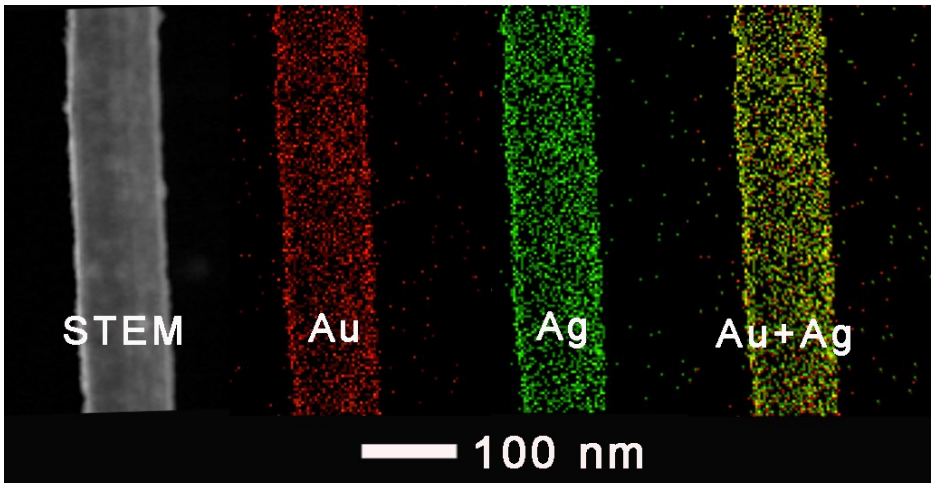

Fig. S6 STEM-EDX mapping images of 1D AgAu alloy nanotrough.

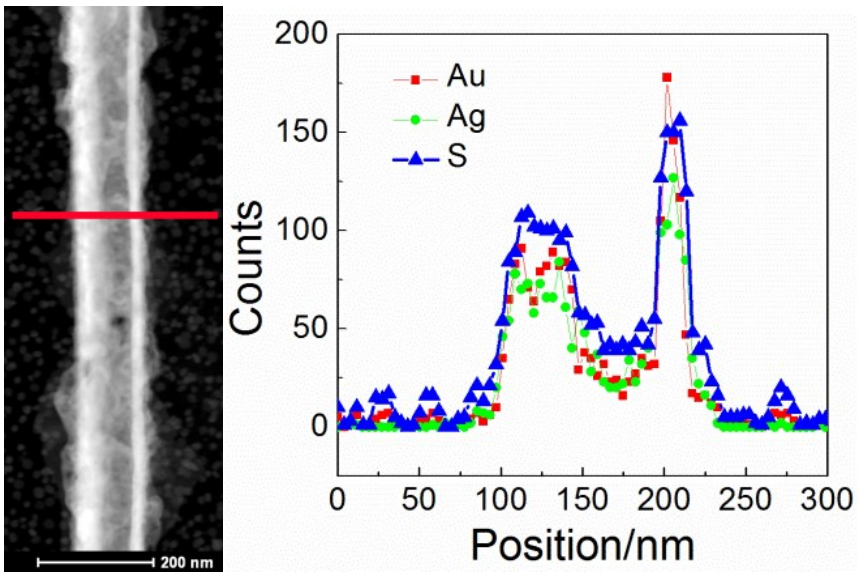

Fig. S7 STEM image and STEM-EDX-linear scan element distribution profile of 1D Au–Ag_2S nanotrough. The element distribution profile indicates that Au, Ag and S had the similar distribution along the transversal direction of a nanotrough, suggesting the formation of a Au/Ag_2S core/shell-like structure.

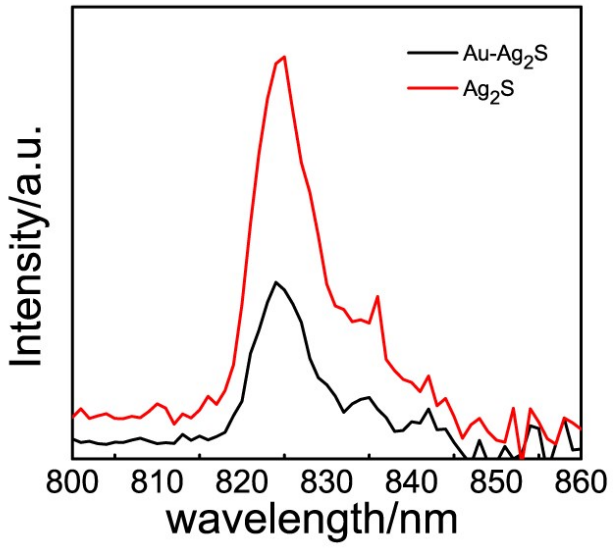

Fig. S8 Photoluminescence (PL) spectra of the pure Ag_2S (red line) and 1D Au-Ag_2S nnaotroughs (black line) (excitation: 550 nm).

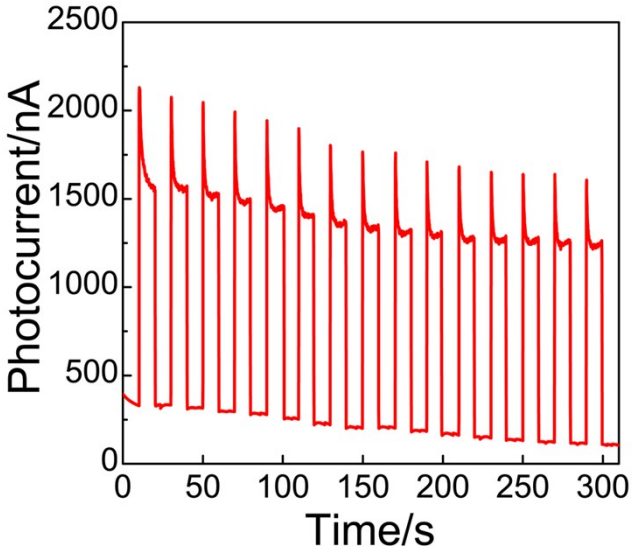

Fig. S9 Photocurrent response of 1D Au-Ag_2S nanotroughs after 15 light on-off cycles. The PEC test was performed in 0.10 mol·L^{-1} Tris–HCl (pH 7.4) containing 0.10 mol·L^{-1} ascorbic acid.

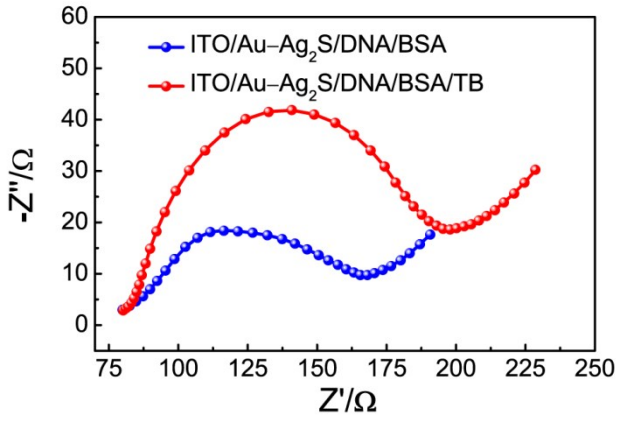

Fig. S10 Electrochemical impedance Nyquist plots of ITO/Au-Ag_2S/DNA/BSA and ITO/Au-Ag_2S/DNA/BSA/TB in 0.1 mol·L^{-1} KCl aqueous solution containing 5.0 mmol·L^{-1} $[Fe(CN)_6]^{3-}$ at −0.22 V (0.1 Hz–100 kHz; amplitude, 5 mV). ITO/Au-Ag_2S/DNA/BSA/TB was obtained by adding 20 μL of 10.0 pmol·L^{-1} human α-thrombin on ITO/Au-Ag_2S/DNA/BSA.

Table S1. Comparison of some methods for TB assay

Methods	System	Detection limit/(pmol L^{-1})	Reference
Photoelectrochemistry	CdS quantum dots	1.0	[4]
Photoelectrochemistry	Graphene-CdS	1.0	[5]
Electrochemistry	Graphene oxide	70.0	[6]
Electrochemistry	Molecular beacon	0.5	[7]
Chemiluminescence	Rolling circle amplification and DNAzyme	6.6	[8]
Fluorescence	Ag nanoparticles (NPs)	3.1	[9]
Electrochemiluminescence	Au NPs–graphene with Ru- thiol-modified biotinylated thrombin aptamer–Au NPs	6.3	[10]
Photoelectrochemistry	1D Au–Ag_2S nanotroughs	0.67	this work

References

[1] H. Y. Shi, B. Hu, X. C. Yu, R. L. Zhao, X. F. Ren, S. L. Liu, J. W. Liu, M. Feng, A. W. Xu and S. H Yu, *Adv. Funct. Mater.*, 2010, **20**, 958-964.

[2] W. C. Geng, W. J. Shen, H. H. Xue, J. L. Sang, L. N. Zhou, X. Yin and Y. J. Li, *ChemNanoMat*, 2019, **5**, 208-214.

[3] L. Cui, J. Hu, M. Wang, X. K. Diao, C. C. Li and C. Y. Zhang, *Anal. Chem.*, 2018, **90**, 11478-11485.

[4] Z. Y. Ma, Y. F. Ruan, N. Zhang, W. W. Zhao, J. J. Xu and H. Y. Chen, *Chem. Commun.*, 2015, **51**, 8381-8384.

[5] S. S. Li, W. Zhu, Y. C. Xue and S. Q. Liu, *Biosens. Bioelectron.*, 2015, **64**, 611-617.

[6] F. Ahour and M. K. Ahsani, *Biosens. Bioelectron.*, 2016, **86**, 764-769.

[7] A. E. Radi, J. L. Acero Sánchez, E. Baldrich and C. K. O'Sullivan, *J. Am. Chem. Soc.*, 2006, **128**, 117-124.

[8] S. Bi, L. Li, and S. S. Zhang, *Anal. Chem.*, 2010, **82**, 9447-9454.

[9] C. F. Jiang, T. T. Zhao, S. Li, N. Y. Gao and Q. H. Xu, *ACS Appl. Mater. Interfaces*, 2013, **5**, 10853-10857.

[10] Y. J. Li, Y. Q. Li, N. Xu, J. H. Pan, T. F. Chen, Y. W. Chen and W. H. Gao, *Sens. Actuators, B*, 2017, **240**, 742-748.